

Up-regulated expression of ADAM17 in gastrointestinal stromal tumors: coexpression with EGFR and EGFR ligands

Motomichi Nakagawa,^{1,5} Kazuki Nabeshima,^{1,6} Shigeyuki Asano,² Makoto Hamasaki,¹ Noriko Uesugi,³ Hiroki Tani,⁴ Yuichi Yamashita⁵ and Hiroshi Iwasaki¹

Departments of ¹Pathology and ⁵Gastroenterological Surgery, Fukuoka University Hospital and School of Medicine, Fukuoka 814-0180; ²Division of Pathology, Iwaki Kyoritsu General Hospital, Iwaki 973-8555; ³Division of Pathology, National Kyushu Medical Center, Fukuoka 810-8563; ⁴Division of Surgery, Hakuai Hospital, Fukuoka 810-0034, Japan

(Received November 3, 2008/Revised December 16, 2008/Accepted December 17, 2008/Online publication March 1, 2009)

Metalloproteinase activities of a disintegrin and metalloproteinases (ADAMs), matrix metalloproteinases (MMPs), and membrane type (MT)-MMPs are involved in many aspects of tumor biology. ADAMs are transmembrane proteins that cleave membrane-anchored proteins to release soluble factors, and thereby mediate important biological phenomena in tumors. The aim of this study was to analyze histopathology, expression and roles of metalloproteinases, especially ADAMs, in gastric gastrointestinal stromal tumor (GIST). Histopathology and immunohistochemical expression of ADAMs were examined in 89 gastric GISTs. In 11 GISTs, ADAM expression was examined at mRNA and protein levels by reverse transcription – polymerase chain reaction (RT-PCR) and immunoblotting, respectively. RT-PCR analysis showed frequent expression of ADAM9 (91%), ADAM10 (64%), ADAM17 (82%), MMP-2 (82%), and MT1-MMP (73%). However, ADAM17 and MMP-2 were the only metalloproteinases that were up-regulated in GISTs at the protein level compared with non-neoplastic gastric tissues. ADAM17 was immunohistochemically expressed in 93% of GIST versus 16% of normal gastric tissues. Furthermore, CD117-positive interstitial cells of Cajal in normal gastric tissues were all negative for ADAM17 with double immunostaining. Expressions of epidermal growth factor receptor (EGFR) and several EGFR ligands such as amphiregulin, heparin-binding epidermal growth factor (HB-EGF), betacellulin, and epiregulin were also demonstrated in GIST by RT-PCR. Protein expression of EGFR, phosphorylated EGFR, amphiregulin, and HB-EGF, both of which can be shed by ADAM17, was confirmed in tumors coexpressing ADAM17 by immunoblotting. Moreover, proteolytically cleaved soluble forms of amphiregulin were identified in tumor extracts. Considered together, the results suggest that ADAM17 may contribute to the progression and growth of GIST through shedding of EGFR ligands and consequent EGFR stimulation. ADAM17, as a major sheddase in GIST, could be potentially a suitable target in anticancer treatment of imatinib-resistant GISTs. (*Cancer Sci* 2009; 100: 654–662)

Gastrointestinal stromal tumors (GISTs) are rare mesenchymal neoplasms of the gastrointestinal tract with an annual incidence of approximately 10–20 per 1 million cases.^(1,2) GISTs express KIT (CD117), a receptor tyrosine kinase encoded by protooncogene *c-kit*. Most of the sporadic GIST cases have somatic gain-of-function mutations of the *c-kit* gene mostly at exon 11, followed by exons 9, 13 and 17.^(3–5) Moreover, a minor subset (approximately 5–7%) of GIST exhibits activating mutations of platelet-derived growth factor receptor- α (PDGFR α) at exons 12, 14 and 18.^(5,6) In the recent past, molecular targeting treatments with imatinib mesylate (STI571), which is a selective inhibitor of ABL (BCR-ABL), KIT, and PDGFR tyrosine kinases, were used in patients with KIT-positive GIST, with significant effectiveness against metastatic

and unresectable GISTs.^(7,8) The antitumor activity of imatinib is heterogeneous, depending on the type of KIT mutation; tumors with KIT exon 11 mutation are more likely to respond to imatinib, while tumors with wild-type KIT or those with other types of mutations are less responsive to imatinib.^(9,10) Thus, further development of new drugs is preferable. Although GISTs exhibit a spectrum of malignant potential behavior, the molecular mechanisms of tumor progression, growth, and invasion have not been fully elucidated. Studies on these mechanisms should provide opportunities to design new molecular therapeutic targets.

Metalloproteinases, such as matrix metalloproteinases (MMPs) and a disintegrin and metalloproteinases (ADAMs) are implicated in various normal and pathophysiological conditions, such as fetal development, cancer development and progression, and inflammatory responses, through proteolysis. Most MMPs are secreted extracellularly except for membrane type (MT)-MMPs, and play a role in tumor biology predominantly by enhancing proteolysis of extracellular matrix macromolecules. On the other hand, ADAMs are a family of genes of multidomain membrane-anchored proteins. They cleave various proteins such as precursors of growth factors and cytokines, receptors, and membrane-anchored proteins to modulate cellular functions.⁽¹¹⁾ Among ADAMs, there is evidence that ADAM17 is an important regulator of growth factor precursor shedding. Although ADAM17 was initially identified as the metalloproteinase responsible for the shedding of tumor necrosis factor α (TNF- α),⁽¹²⁾ it is also necessary for the shedding of several epidermal growth factor receptor (EGFR) ligands including transforming growth factor α (TGF- α), heparin-binding epidermal growth factor (HB-EGF), and amphiregulin.^(13,14)

To our knowledge, there is little or no information on the expression of ADAMs and their roles in gastric GISTs. In the present study, we investigated the expression of ADAMs and MMPs in gastric GISTs. The results showed preferential up-regulation of ADAM17 in GISTs, relative to non-neoplastic gastric tissues. The interstitial cells of Cajal in non-neoplastic tissues did not express ADAM17 immunohistochemically. Moreover, EGFR expression with its phosphorylated forms and expression of ADAM17-sensitive EGFR ligands, amphiregulin and HB-EGF, including their shed forms, were also found in GISTs. This is the first study to suggest possible involvement of EGFR and ADAM17-mediated EGFR ligand shedding in tumor growth of gastric GIST.

⁶To whom correspondence should be addressed. E-mail: kaznabes@fukuoka-u.ac.jp

Materials and Methods

Patients. This study analyzed 89 GISTs that were obtained from pathology files at Fukuoka University Hospital in Fukuoka, Japan and Iwaki Kyoritsu General Hospital in Iwaki, Japan, between 1989 and 2006. Anonymous use of redundant tissue is part of the standard treatment agreement with patients in these hospitals when no objection is expressed. Clinical information concerning the sites of the lesion and the sizes of the tumor were obtained from reviewing the medical records. None of these patients underwent radiotherapy or chemotherapy before surgery. Histological diagnosis of GIST was established based on the histological features and immunohistochemical expression of KIT and/or CD34.⁽¹⁾ The histopathological findings, including tumor size, hemorrhage, necrosis, cell types (spindle, epithelioid, or mixed type), and mitotic counts per 50 high power fields (hpf) were evaluated in each tumor by reviewing the hematoxylin and eosin-stained sections. GISTs were classified into very low-, low-, intermediate-, and high-risk groups regarding their estimated potential for aggressive clinical behavior as proposed in the consensus report of the National Institutes of Health (NIH) GIST Workshop in April 2001.⁽²⁾

Immunohistochemistry. Immunohistochemical staining of formalin-fixed, paraffin-embedded tissue sections was performed using a biotin-streptavidin method. Heat-induced antigen retrieval was employed for ADAM17, KIT, CD34, and desmin. Polyclonal antibodies (poly Ab) against KIT (CD117) (Immuno-Biological Laboratory, Fujioka, Japan), S-100 protein (Dako Cytomation, Glostrup, Denmark), and ADAM17 (Calbiochem, Darmstadt, Germany) and monoclonal antibodies (mAb) against CD34 (QBEND10, Immuno-Biological Laboratory), α -smooth muscle actin (α -SMA; 1A4, Dako), and desmin (D33, Dako) were used. Immunoreactions were revealed with alkaline phosphatase or horseradish peroxidase activity using naphthol-AS-BI-phosphate or Metal-3,3'-diaminobenzidine as a substrate, respectively.

The immunohistochemical specificity of the antibody was confirmed by two types of negative controls: substituting mouse (for mAb) or rabbit (for poly Ab) non-immune IgG for the primary antibody and omitting the primary antibody in the staining protocol. Immunostaining was considered negative if stained tumor cells were less than 10%. In specimens considered positive, staining of the tumor was scored based on the percentage of positive tumor cells as 1+ (10–50% of cells positive) or 2+ (>50% of cells positive).

Double immunostaining for KIT and ADAM17 was performed using Envision labeled polymer reagent (DAKO) and a biotin-streptavidin method. First, sections were stained for KIT. After non-specific sites were blocked as described earlier, the sections were incubated with anti-KIT poly Ab (Immunobiological Laboratory) for 1 h at room temperature. The sections were then washed in total serum bilirubin (TBS), and incubated with Envision reagent for 30 min at room temperature (RT). The attached antibody was visualized by 3,3'-diaminobenzidine. The primary and secondary antibodies were removed from tissue by washing in three changes of 0.1 M glycine-HCl (pH 2.2) for 1 h. Then, the biotin-streptavidin method was repeated using anti-ADAM17 mAb (Calbiochem) as described earlier. The reaction was revealed with naphthol AS-BI phosphate and counterstained with methyl green.

Detection of metalloproteinases, growth factor receptors, and their ligands by Western blotting. Proteins including ADAMs, MMPs, and EGFR ligands were extracted from tissue samples using a homogenizer (polytron-aggregate; Kinematica, Luzern, Switzerland) in a lysis buffer containing 10 mM Tris-HCl (pH 7.5), 150 mM NaCl, 2 mM ethylenediaminetetraacetic acid (EDTA), 1% Triton X-100 and protease inhibitors (Complete Mini, Roche Applied Sciences, Penzberg, Germany) on ice for

30 min. The extracts were clarified by centrifugation at $18\,000 \times g$ for 10 min, and subjected to sodium dodecyl sulfate-polyacrylamide gel electrophoresis (SDS-PAGE) after measurement of their protein concentrations using the Bio-Rad (Hercules, CA, US) protein assay. After electrophoresis, the proteins were transferred electrophoretically to Immobilon membrane (Millipore, Bedford, MA, US). Nonspecific sites were blocked with 5% non-fat dry milk in 0.05% Tween-20/0.05 M Tris-buffered saline (pH 7.6) (TBS-T) at 37°C for 1 h and the membrane was incubated overnight at 4°C with mAb against MMP-2 (75-7F7, Daiichi Fine Chemical, Toyama, Japan), MT1-MMP (114-6G6, Daiichi Fine Chemical), and EGFR (H11, Dako) and poly Ab against ADAM17 (Calbiochem), ADAM9 (R & D Systems, Wiesbaden, Germany), ADAM10 (Chemicon International, Temecula, CA), HB-EGF (R & D Systems), amphiregulin (ThermoFisher Scientific, Cheshire, UK), and α -tubulin (Cell Signaling Technology, Danvers, MA). After washing with TBS-T, the membrane was incubated for 1 h with peroxidase-conjugated goat antimouse or goat antirabbit IgG. Reactions were revealed with chemiluminescence reagents (DuPont NEN, Boston, MA, US) according to the manufacturer's instructions. The membranes were exposed to X-ray film, and the bands on the film were subjected to image analysis (NIH ImageJ version 1.37). Statistical analysis was performed using Student's *t*-test.

Detection of phosphorylated EGFR by Western blotting. Proteins including phosphorylated EGFR (pEGFR) were extracted from tissue samples using a homogenizer in a lysis buffer containing 50 mM Tris-HCl (pH 7.4), 150 mM NaCl, 1 mM EDTA, 1 mM Na_3VO_4 , 1% Triton X-100 and protease inhibitors (Complete Mini) on ice for 30 min. After sonication and centrifugation, the extracts were subjected to SDS-PAGE. Immunoblotting was performed as described earlier except for blocking of non-specific sites by 2% bovine serum albumin (BSA) in TBS-T and incubation with antiEGFR poly Ab (Santa Cruz Biotechnology, Santa Cruz, CA, US).

RNA extraction and reverse transcription-polymerase chain reaction (RT-PCR) analysis. mRNA was isolated from fresh frozen tissue of original tumors, using a QuickPrep Micro mRNA Purification Kit (Amersham Biosciences, Piscataway, NJ) according to the protocols provided by the manufacturer. Next, 1 μg of mRNA from each sample was reverse-transcribed using Ready-To-Go T-primed First-Strand Kit (Amersham Biosciences). PCR amplifications were performed with puReTaq Ready-To-Go PCR Beads (Amersham Biosciences). Primer pairs are listed in Table 1. Reaction mixtures were initially denatured at 95°C for 3 min, followed by 35 cycles of 1 min at 95°C, 1 min at the respective annealing temperature (Table 1), and 1 min at 72°C in a thermal cycler (GeneAmp[®] PCR System 9700, PE Applied Biosystems, Foster City, CA). Finally, 6 μL of the PCR products were analyzed by electrophoresis on 2% agarose gel stained with ethidium bromide.

Statistical analysis. Summary statistics were obtained using established methods and statistical analysis software StatView for Windows version 5.0 (SAS Institute Inc., Cary, NC, US). The relationships between several clinicopathological parameters and histopathological subgroups were evaluated using the χ^2 test and Fisher's exact test. A *P*-value of <0.05 was considered statistically significant.

Results

Clinicopathological findings. The clinicopathological characteristics of the 89 patients are summarized in Table 2. Tumors had an average size of 4.9 ± 4.7 cm, ranging from 0.1 to 27 cm. Macroscopically, the tumors were relatively well circumscribed and showed partially lobulated appearance. Hemorrhage and necrosis were focally noted (42% and 20%, respectively; Table 2).

Table 1. Primers for reverse transcription – polymerase chain reaction

Name		Oligonucleotide sequence	AT (°C)	Product size	Reference
ADAM8	Forward	5'-GCCGTCTTCAGGCCTCGGCCGGGACTCT-3'	54	651 bp	(39)
	Reverse	5'-AGGGGCGTTGGCGAGGCACACCGACTGCGG-3'			
ADAM9	Forward	5'-GCTGTCTTGCCACAGACCCGGTATGTGGAG-3'	67	604 bp	(39)
	Reverse	5'-TGGAATATTAAGAAGGCAGTTTCTCTTT-3'			
ADAM10	Forward	5'-ATCCAGTCATGTAAAGCGATTGATACAATTTAC-3'	60	434 bp	(39)
	Reverse	5'-TCCAAAGTTATGTCCAACCTCGTGAGCAAAAGTAA-3'			
ADAM12 s	Forward	5'-GCACCTCCCTTCTGTGACAAGTTT-3'	60	504 bp	(39)
	Reverse	5'-TGAAAGGCCAGACTTTTGAGTCT-3'			
ADAM12 m	Forward	5'-GCACCTCCCTTCTGTGACAAGTTT-3'	56	643 bp	(39)
	Reverse	5'-CTTGGTGTGGATATTGTGGAGCAG-3'			
ADAM15	Forward	5'-CTGGGACAGCGCCACATTCGCCGGAGGCGG-3'	67	688 bp	(39)
	Reverse	5'-TCCGCAGAAAGCAGCCATAGGGGGTAGGCT-3'			
ADAM17	Forward	5'-AGAGCTGACCCAGATCCCATGAAGAACAGC-3'	67	777 bp	(39)
	Reverse	5'-GCGTCTTGAAAACACTCCTGGGCCTTACT-3'			
ADAM19	Forward	5'-TGTGGGAAGATCCAGTGA-3'	60	500 bp	(39)
	Reverse	5'-AGAGCTGAGGGCTTGAGTTG-3'			
ADAM20	Forward	5'-AAAATAGCACACAGATGGAGTTGCAATTG-3'	60	702 bp	(39)
	Reverse	5'-ATCCACAGTACTTCAGTCTAAATATATT-3'			
ADAM21	Forward	5'-TCTGGCTTGGGGTATTTTG-3'	60	500 bp	(39)
	Reverse	5'-TTGGCGTGCTACTTCCTTCT-3'			
ADAM28 s	Forward	5'-GCTGTGATGCTAAGACATGT-3'	60	644 bp	(39)
	Reverse	5'-GTTTATGATCTTAGTAGGGTTGCC-3'			
ADAM28 m	Forward	5'-GCTGTGATGCTAAGACATGT-3'	60	871 bp	(39)
	Reverse	5'-TGAACAGCCTTACCATCG-3'			
ADAM30	Forward	5'-AACCAGGTGCCAACTGTAGC-3'	60	496 bp	(39)
	Reverse	5'-CCCATGGGTTTCATGGATAG-3'			
MMP-1	Forward	5'-CGACTCTAGAAACACAAGAGCAAGA-3'	57	786 bp	(40)
	Reverse	5'-AAGGTTAGCTTACTGTCACACGCTT-3'			
MMP-2	Forward	5'-GTGCTGAAGGACACACTAAAGAAGA-3'	57	580 bp	(40)
	Reverse	5'-TTGCCATCCTTCTCAAAGTTGTAGG-3'			
MMP-3	Forward	5'-AGATGCTGTTGATTCTGCTGTTGAG-3'	57	515 bp	(40)
	Reverse	5'-ACAGCATCAAAGGACAAAGCAGGAT-3'			
MMP-7	Forward	5'-AAACTCCCGCTCATAGAAAT-3'	57	394 bp	(41)
	Reverse	5'-TCCCTAGACTGCTACCATCCG-3'			
MMP-9	Forward	5'-CACTGTCCACCCCTCAGAGC-3'	61	243 bp	(40)
	Reverse	5'-GCCACTTGTCCGCGATAAGG-3'			
MMP-10	Forward	5'-CACTCTACAACTCATTACAGAGCT-3'	57	408 bp	(40)
	Reverse	5'-CTTGGATAACCTGCTGTACCTCAT-3'			
MMP-13	Forward	5'-CCTGGCTGCCTTCTCTTCTTGA-3'	57	280 bp	(42)
	Reverse	5'-AACCCCGCATCTTGGCTTTTTTC-3'			
MT1-MMP	Forward	5'-TCGGCCCAAAGCAGCAGCTTC-3'	59	180 bp	(43)
	Reverse	5'-CTTCATGGTGTCTGCATCAGC-3'			
MT2-MMP	Forward	5'-CAGCCAGCCGCCATATGTC-3'	59	169 bp	(43)
	Reverse	5'-CTTCACTCGTACCCCGAAC-3'			
MT3-MMP	Forward	5'-ACAGTCTGCGGAAACGGAGCAG-3'	57	185 bp	(43)
	Reverse	5'-GTCAATTGTGTTTCTGTCCAC-3'			
TGF- α	Forward	5'-TCAGTCTGCTCCATGCAACC-3'	59	317 bp	(44)
	Reverse	5'-TTTCTGAGTGGCAGCAAGCG-3'			
EGF	Forward	5'-TGCAACTGTGTTGTTGGCTACATC-3'	58	339 bp	(44)
	Reverse	5'-TGGTTGACCCCATCTTGTAG-3'			
HB-EGF	Forward	5'-ACAAGCACTGGCCACACCAAACAAG-3'	52	299 bp	(39)
	Reverse	5'-CCACGATGACCAGCAGACAGACAGA-3'			
Amphiregulin	Forward	5'-AGAGTTGAACAGGTAGTTAAGCCCC-3'	54	421 bp	(44)
	Reverse	5'-GTCGAAGTTTCTTTCGTTCTCAG-3'			
Betacellulin	Forward	5'-TTCATGTGTGGTGGCAGATGG-3'	57	350 bp	(44)
	Reverse	5'-ACAGCATGTGCAGACCCGATG-3'			
Epiregulin	Forward	5'-ATCATGTATCCCAGGAGTCCAG-3'	54	263 bp	(44)
	Reverse	5'-GAATCACGGTCAAAGCCACATAC-3'			
EGFR	Forward	5'-GAGAGGAGAACTGCCAGAA-3'	53	454 bp	(45)
	Reverse	5'-GTAGCATTTATGGAGAGTG-3'			
HER2	Forward	5'-AGGGAAACCTGGAATCACC-3'	55	296 bp	(46)
	Reverse	5'-TGGATCAAGACCCCTCCTT-3'			
HER3	Forward	5'-CAGGTGCTGGGCTTGCTTTT-3'	55	366 bp	(46)
	Reverse	5'-GTGGCTGGAGTTGGTGTAT-3'			
HER4	Forward	5'-TCCAGCCCAGCGATTCTCAG-3'	55	495 bp	(46)
	Reverse	5'-GGCCAGTACAGGACTTATGG-3'			
G3PDH	Forward	5'-TCCACCACCTGTTGCTGTA-3'	60	450 bp	(45)
	Reverse	5'-ACCACAGTCCATGCCATCAC-3'			

AT, annealing temperature; ADAM, a disintegrin and metalloproteinase; MMP, matrix metalloproteinase; TGF- α , tumor growth factor alpha; EGF, epidermal growth factor; HB-EGF, heparin binding epidermal growth factor; EGFR, epidermal growth factor receptor; HER, human epidermal growth factor receptor; G3PDH, glyceraldehyde-3-phosphate dehydrogenase.

Table 2. Clinicopathological details for gastric gastrointestinal stromal tumor (GIST) (n = 89)

Variable	n (%)	Mean ± SEM (range)
Gender		
Male	49 (55.1)	
Female	40 (44.9)	
Age (years)		65.2 ± 1.2 (29–87)
Tumor		
Size (cm)		4.9 ± 4.7 (0.1–27)
Necrosis	20 (22)	
Hemorrhage	42 (47)	
Mitotic index (mf/50 hpf)		12.1 ± 2.5 (0–149)
Immunohistochemistry		
CD117	89 (100)	
CD34	86 (97)	
α-SMA	22 (25)	
Desmin	4 (5)	
S-100 protein	2 (2)	

α-SMA, α-smooth muscle actin; mf, mitotic figures.

Histologically, 76 tumors (85%) were of spindle cell type, seven (8%) of epithelioid cell type, and the remaining six (7%) revealed mixed histology with both spindle and epithelioid components. Immunohistochemically, all 89 GISTs were KIT-positive (100%), 86 (97%) CD34-positive, 22 (25%) positive for α-SMA, four (5%) for desmin, and two (2%) for S-100 protein. Tumors were classified into very low- (21/89, 24%), low-

(23/89, 26%), intermediate- (14/89, 15%), and high-risk (31/89, 35%) groups according to the NIH consensus meeting report (Table 3).

mRNA expression of ADAMs, MMPs, and MT-MMPs in GISTs. To determine which types of the metalloproteinases are expressed in GIST, we performed RT-PCR using 23 primer pairs listed in Table 1. mRNA was obtained from 11 GISTs, including four of the very low/low-risk group and seven of the high-risk group, and three non-neoplastic gastric tissues. The mRNA expression was detected for all the metalloproteinase species except for ADAM8, ADAM12s, ADAM15, ADAM20, ADAM21, MMP-7, MMP-13, and MT2-MMP at least in one of the tissues examined (Fig. 1). ADAM9 expression was most frequently observed (10/11, 91%), followed by expression of ADAM17 (9/11, 82%), MMP-2 (9/11, 82%), MT1-MMP (8/11, 73%), and ADAM10 (7/11, 64%). Thus, we focused on these ADAMs (9, 10, and 17), MMP-2, and MT1-MMP, and further analyzed their protein expression levels.

Protein expression of ADAMs, MMPs, and MT-MMPs in GISTs. Protein expression levels of the above selected metalloproteinases were examined using Western blotting in seven GISTs (3 of the very low/low-risk group and 4 of the high-risk group) and two non-neoplastic gastric tissues. All tumors expressed both the 115-kDa pro-form and the 90-kDa active form of ADAM17 (Fig. 2). Semi-quantitative analysis demonstrated that both pro- and active forms were expressed at higher levels in tumors compared with those in non-neoplastic tissues (Fig. 3a). The total expression levels (sum of pro- and active forms) were significantly higher in tumors than non-neoplastic tissues (3–3.5 times higher in tumors), whereas the difference between the

Table 3. Risk grades of gastrointestinal stromal tumor (GIST) and clinicopathological details

Classification based on risk grades ^a (size, mitotic count)	n (%)	Size in cm median (range)	Mitotic count mf/50 hpf (range)
Very low risk (<2 cm, <5/50 hpf)	21 (24)	0.9 (0.1–1.9)	0.4 (0–4)
Low risk (2–5 cm, <5/50 hpf)	23 (26)	3.4 (2.5–4.5)	1.9 (0.4)
Intermediate risk (<5 cm, 6–10/50 hpf) (5–10 cm, <5/50 hpf)	14 (15)	5.9 (2.5–9.0)	3.1 (0–8)
High risk (>5 cm, >5/50 hpf, >10 cm or >10/50 hpf)	31 (35)	8.4 (2.5–27)	31.6 (3–149)

^aFletcher CD *et al.* 2002. hpf, high power field; mf, mitotic figures.

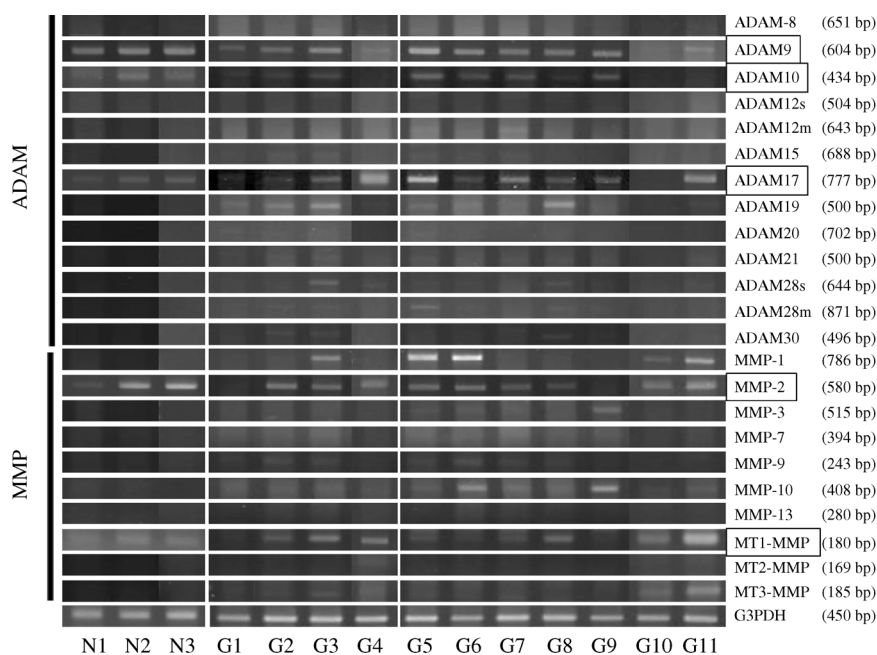


Fig. 1. Reverse transcription – polymerase chain reaction detection of a disintegrin and metalloproteinase (ADAM) and matrix metalloproteinase (MMP) expression in 11 gastrointestinal stromal tumors (GISTs) and 3 non-neoplastic gastric tissues. G1–4, GIST of the very low/low risk group; G5–11, GIST of the high risk group, N1–3, non-neoplastic gastric tissue. G3PDH, glyceraldehyde-3-phosphate dehydrogenase.

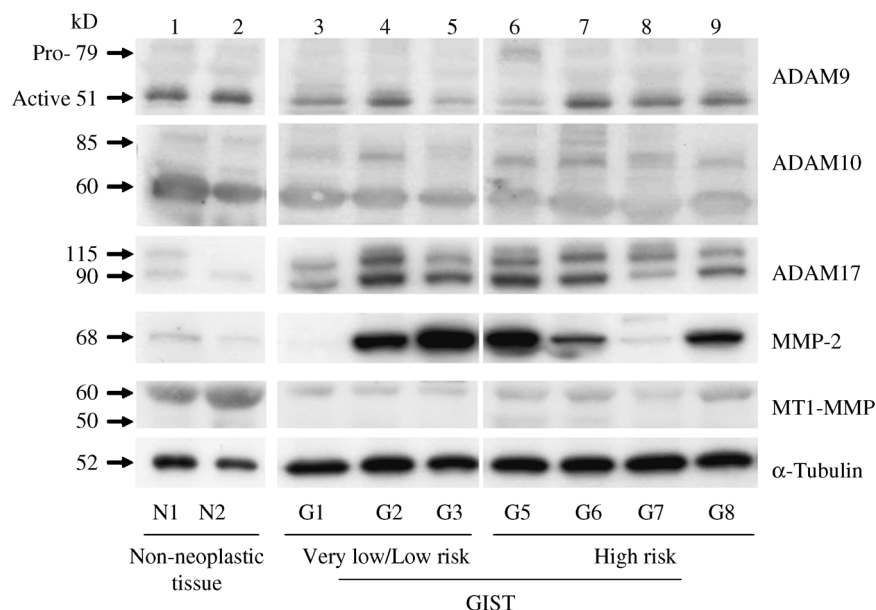


Fig. 2. Immunoblot analysis of a disintegrin and metalloproteinases (ADAM)9, 10, and 17, matrix metalloproteinase (MMP)-2, and MT1-MMP. Tissue extracts were subjected to immunoblot analysis with antibodies to ADAM9, 10, and 17, MMP-2, MT1-MMP, and α -tubulin, as described in the Materials and Methods section. Bands at 79 and 51 kDa for ADAM9, 85 and 60 for ADAM10, and 115 and 90 for ADAM17 correspond to the proform and active form, respectively. Bands at 68 kDa correspond to proMMP-2, and those at 60 and 50 kDa for MT1-MMP correspond to its pro- and active forms, respectively.

Table 4. Risk grades of gastrointestinal stromal tumor (GIST) and a disintegrin and metalloproteinase (ADAM)17 immunohistochemistry

	Total	0	1+	2+	Positive rate (%)	Rate of 2+ (%)
Normal	49	41	8	0	16.3 [†]	0
KIT-positive ICC [‡]		49	0	0	0	0
Gastric GIST	80	6	12	62	93.8*	78.8
Very low risk	17	4	3	10	76.5	58.8
Low risk	21	1	1	19	95.2	90.5
Intermediate risk	14	1	3	10	92.9	78.6
High risk	28	0	5	23	100	82.1

Immunohistochemical expression of ADAM17 was graded as 0 (<10% of cells positive), 1+ (10–50%), and 2+ (>50%). ICC, the interstitial cells of Cajal.

[†]Fisher's exact test, $P < 0.001$.

[‡]ADAM17 expression in ICC was determined by double immunostaining for CD117 (KIT) and ADAM17.

Table 5. A disintegrin and metalloproteinase (ADAM)17 immunohistochemistry and histopathological characteristics

Gastric GIST	Total (80)	0 (6)	1+ (12)	2+ (62)	Positive rate (%)	Rate of 2+ (%)
Cell type						
Spindle	69	5	10	54	93	78
Epithelioid	6	1	1	4	83	67
Mixed	5	0	1	4	100	80
Necrosis						
+	18	0	2	16	100	89
-	62	6	10	46	90	74
MF						
<5/50	49	5	7	37	90	76
≥5/50	31	1	5	25	97	81
Size (cm)						
<5	48	6	5	37	88	77
≥5	31	0	6	25	100	81

GIST, gastrointestinal stromal tumor; MF, mitotic figure.

tumors of the very low/low-risk and the high risk groups was not statistically significant (Fig. 3b). The expression level of 68-kDa proform of MMP-2 was also higher in tumors than non-neoplastic tissues (Fig. 2). However, the expression levels of ADAM9, ADAM10, and MT1-MMP were similar in non-neoplastic and tumor tissues.

Immunohistochemistry for ADAM17. Since immunoblot analysis revealed increased expression of ADAM17 in GISTs, we next examined the expression of ADAM17 immunohistochemically in 80 GIST and 49 non-neoplastic gastric tissues including interstitial cells of Cajal. GIST cells expressed ADAM17 in their cytoplasm or along the cell membrane (Fig. 4a–c), while the non-neoplastic proper muscle layer rarely stained positive (Fig. 4c). To confirm the up-regulation of ADAM17 in GIST, we examined ADAM17 expression in interstitial cells of Cajal by using double immunostaining for KIT and ADAM17. Cajal cells with delicate bipolar cytoplasmic projections, which were identified by KIT reactivity, were negative for ADAM17 in all non-neoplastic tissues (Fig. 4e, Table 4), while GIST cells expressed both KIT and ADAM17 (Fig. 4f). The results are summarized in Table 4. ADAM17 was positive in 74/80 (93%) cases of GIST, and 62/80 cases (78%) showed 2+ (>50%) expression. Only 8/49 (16%) non-neoplastic gastric tissues were positive for ADAM17, with no 2+ cases. The difference in positivity between GIST and non-neoplastic tissues was significant ($P < 0.001$, Table 4). Among the different risk groups of GIST, although ADAM17 expression levels tended to be lower in the very low-risk group (2+, 59%) compared with low- (2+, 91%), intermediate- (2+, 79%), and high- (2+, 82%) risk groups, the difference was not statistically significant. ADAM17 expression levels were not significantly different in relation to histological cell types, presence or absence of necrosis, mitotic counts, and the tumor size (Table 5). In the present study, GIST recurred in five cases. ADAM17

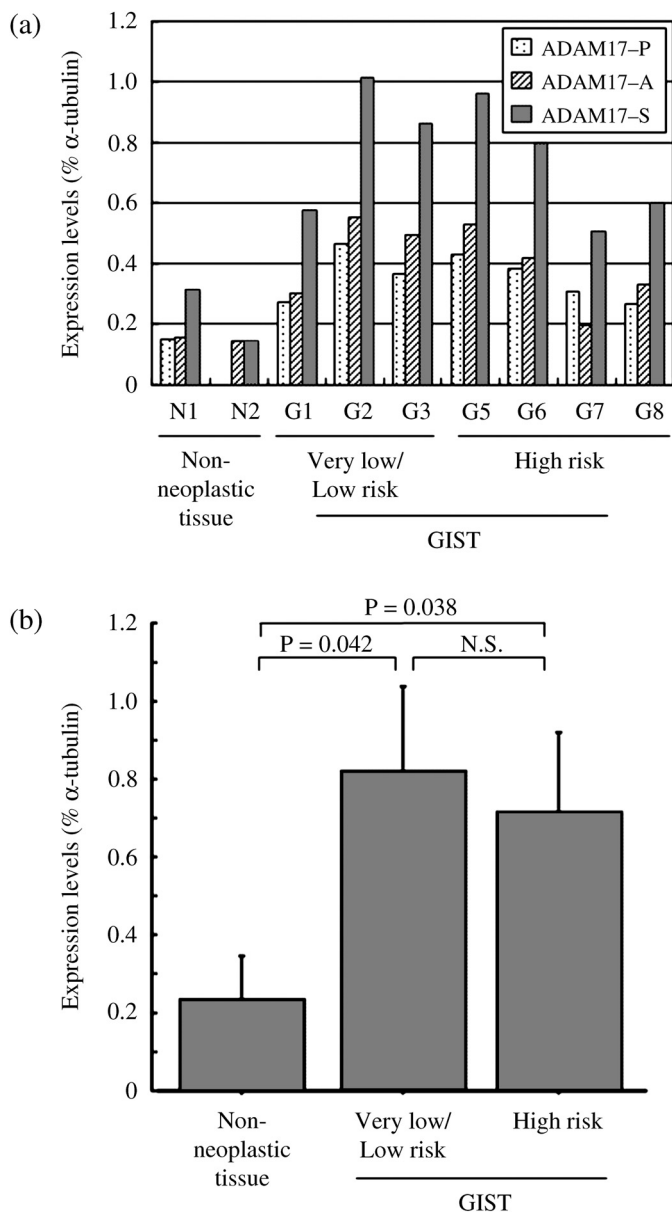


Fig. 3. Semiquantitative analysis of a disintegrin and metalloproteinase (ADAM)17 protein expression. After immunoblotting, the bands on the film were subjected to image analysis as described in the Materials and Methods section. The expression level is depicted relative to that of α -tubulin in each tumor. (a) Relative expression levels of the proform (ADAM17-P), active (ADAM17-A) forms, and the sum of pro- and active forms (ADAM17-S). (b) Relative expression levels of ADAM17, as a sum of pro- and active forms, in non-neoplastic tissues ($n = 2$), gastrointestinal stromal tumor (GIST) of the very low/low risk group ($n = 3$), and GIST of the high risk group ($n = 4$). Data are mean \pm SEM.

immunohistochemistry was available in 4/5 cases, and all four cases showed high ADAM17 expression (2+).

Expression of EGFR and EGFR ligands.

RT-PCR studies. Since most GIST (94%) expressed ADAM17 that can cleave and shed some EGFR ligands, we examined the expression of EGFR species (HER1–4) and EGFR ligands (EGF, TGF- α , betacellulin, amphiregulin, epiregulin, and HB-EGF) by RT-PCR in 11 GIST and three non-neoplastic gastric tissues. Among EGFR species, EGFR (HER1) was the most frequently expressed in GISTs (8/11, 73%), followed by

HER4 (5/11, 45%) and HER2 (4/11, 36%) (Fig. 5). HER3 was undetectable. Of the EGFR ligands, expressions of amphiregulin, HB-EGF, betacellulin, and epiregulin were detected in 10/11 (91%), 9/11 (82%), 9/11 (82%), and 8/11 (73%) cases of GIST, respectively. EGF and TGF- α were undetectable.

Immunoblotting studies. Among the frequently expressed EGFR ligands, amphiregulin and HB-EGF can be cleaved and shed by ADAM17. Thus, we examined the protein expression of these ligands as well as pEGFR by Western blotting in seven GIST and two non-neoplastic tissues. Expression of pEGFR, depicted as a band at 170 kDa,⁽¹⁵⁾ was found in all six tumors examined (Fig. 6). Of the EGFR ligands, the 30 kDa form of HB-EGF was expressed in all tumors and non-neoplastic tissues. Faint bands of the 22-kDa form were also detected in some tumors. Both the 30 and 22 kDa forms correspond to the transmembrane forms of proHB-EGF.⁽¹⁶⁾ Five of seven GISTs and two of two non-neoplastic tissues expressed amphiregulin. However, the expressed forms were different between tumor and non-neoplastic tissues; tumors exhibited five bands at 50, 43, 28, 22, and 19 kDa, whereas non-neoplastic tissues expressed only the 50-kDa form. Bands at 50 kDa in tumors were very faint. Bands at 50 and 28 kDa correspond to the transmembrane forms of pro-amphiregulin, while the 43, 22, and 19-kDa forms correspond to shed, soluble forms of amphiregulin.⁽¹⁷⁾

Discussion

The present study provided the first evidence of up-regulation of ADAM17 in gastric GISTs. Phosphorylated EGFR and EGFR ligands that can be shed by ADAM17 were coexpressed in many of the tumor tissues expressing ADAM17 (Figs 2 and 6, in 6/7 [86%] of tumors). Shed forms of amphiregulin, one of ADAM17-sensitive EGFR ligands, were detected in tumor extracts. These findings suggest that ADAM17 may contribute to the progression and growth of gastric GIST via EGFR–EGFR ligand interaction. Since primary and acquired resistance to imatinib is an increasing clinical problem at present,⁽¹⁰⁾ the identification of ADAM17 as a major sheddase in gastric GISTs further expands the potential of ADAM17 as a potentially suitable target in anticancer treatment of imatinib-resistant GISTs.

In the present study, only ADAM17 and MMP-2 were up-regulated at the protein level in GISTs compared with their expression in normal tissues. Co-expression of MMP-2 and MT1-MMP, an activator of proMMP-2, in these tumors suggest that MMP-2 may play a role in tumor invasion in gastric GISTs. ADAM17 was frequently expressed in GISTs, and the immunohistochemical expression level was high (2+, >50%) in 78% (62/80) of cases. Similarly, over-expression of ADAM17 has been reported in cancers of the stomach, breast, colon, ovary, and prostate, and also cell lines derived from leukemia and prostate cancer.^(11,18–21) ADAM17, also known as TNF- α -converting enzyme, is one of the best-characterized members of the ADAM family of proteins and has a broad role in ectodomain shedding. The substrates of ADAM17 mediated shedding include ligands of EGFR such as TGF- α , HB-EGF, and amphiregulin.^(13,14) The potential importance of ADAM17 in EGFR ligand shedding was demonstrated through a germ line mutation in mice that eliminated the zinc-binding domain (*Tace* ^{Δ Zn}), thereby inactivating the protease.⁽²²⁾ *Tace* ^{Δ Zn/ Δ Zn} mice exhibited skin and eye defects identical to those observed in mice lacking TGF- α ,⁽²³⁾ and defective in shedding of TGF- α was noted in *Tace*^{Zn/Zn} mice-derived cells.⁽²²⁾ Moreover, ADAM17-deficient mice died perinatally, exhibiting widespread epithelial defects reminiscent of EGFR-deficient mice.⁽²⁴⁾ These observations suggest that ADAM17 acts as a regulator of the availability of EGF family ligands. Frequent and diffuse expression of ADAM17 in GISTs suggests its role as a sheddase in GIST tumorigenesis.

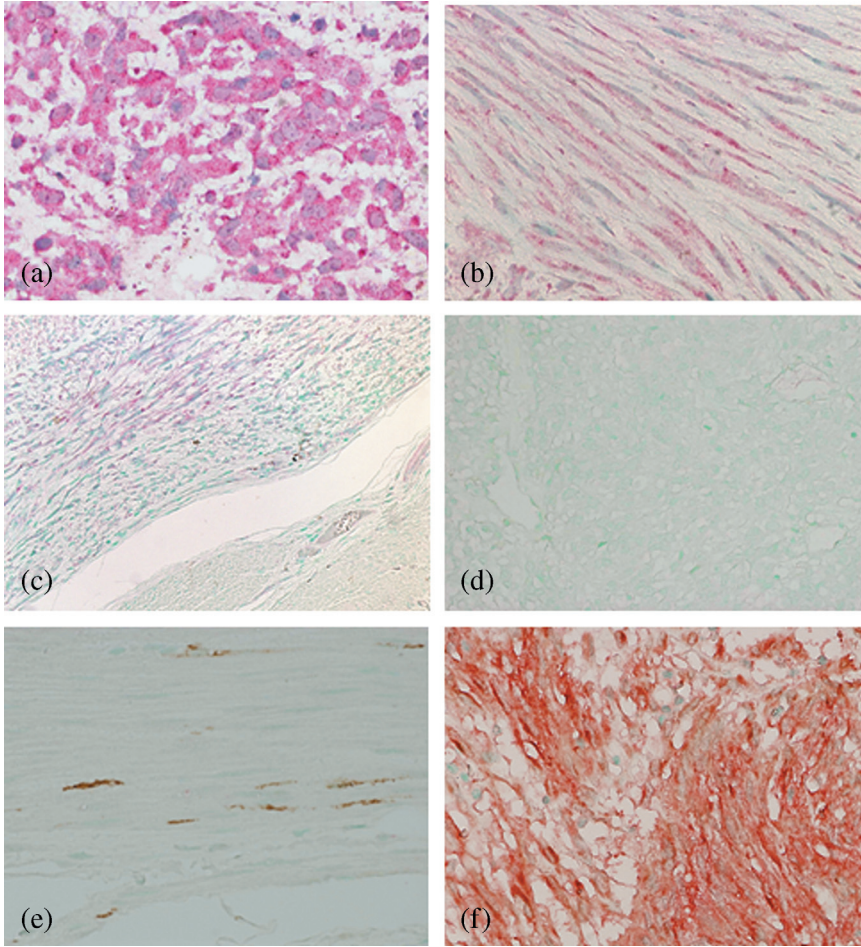


Fig. 4. A disintegrin and metalloproteinase (ADAM)17 immunohistochemistry in gastrointestinal stromal tumor (GIST) and interstitial cells of Cajal. (a) Epithelioid type. ADAM17 reactivity is demonstrated in the cytoplasm and along the cell membrane (inset). (b) Spindle cell type. ADAM17 is expressed in spindle-shaped cytoplasm. (c) Tumor border. Tumor cells are positive for ADAM17, while cells of the non-neoplastic proper muscle layer are negative. (d) Negative control. ADAM17 expression in interstitial cells of Cajal was examined by double immunostaining for KIT (CD117) (brown) and ADAM17 (red) (e, f). (e) The interstitial cells of Cajal identified by immunoreactivity for KIT are negative for ADAM17. The cells have delicate bipolar cytoplasmic projections. (f) Most of GIST cells stain red-brown, indicating immunoreactivity for both KIT and ADAM17. (a-d) immunostaining for ADAM17 (e, f) double immunostaining for KIT and ADAM17.

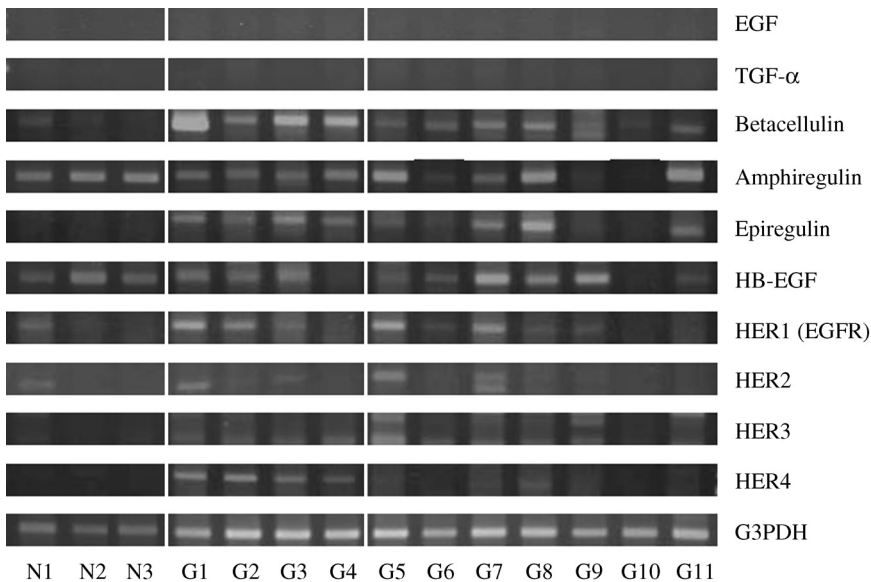


Fig. 5. Reverse transcription – polymerase chain reaction detection of epidermal growth factor receptor (EGFR) and EGFR ligand species in 11 gastrointestinal stromal tumors (GISTs) and three non-neoplastic gastric tissues. G1–4, GIST of the very low/low risk group; G5–11, GIST of the high risk group, N1–3, non-neoplastic gastric tissue. EGF, epidermal growth factor; TGF- α , transforming growth factor- α ; HB-EGF, heparin binding epidermal growth factor; HER1–4, human epidermal growth factor receptor type 1–4; G3PDH, glyceraldehyde-3-phosphate dehydrogenase.

GIST is believed to originate from interstitial cells of Cajal or their stem cell-like precursors.⁽⁴⁾ Optically, normal Cajal cells should be analyzed as control; however, these cells are difficult to separate from the smooth muscle cells of the gastrointestinal wall and there are no Cajal cell lines available for culture. In the

present study, although tumor tissues were compared with non-neoplastic gastric tissues to examine frequently expressed MMPs and ADAMs, we confirmed the up-regulation of ADAM17 in GIST by double immunostaining for KIT and ADAM17. KIT-positive interstitial cells of Cajal in 49 non-neoplastic

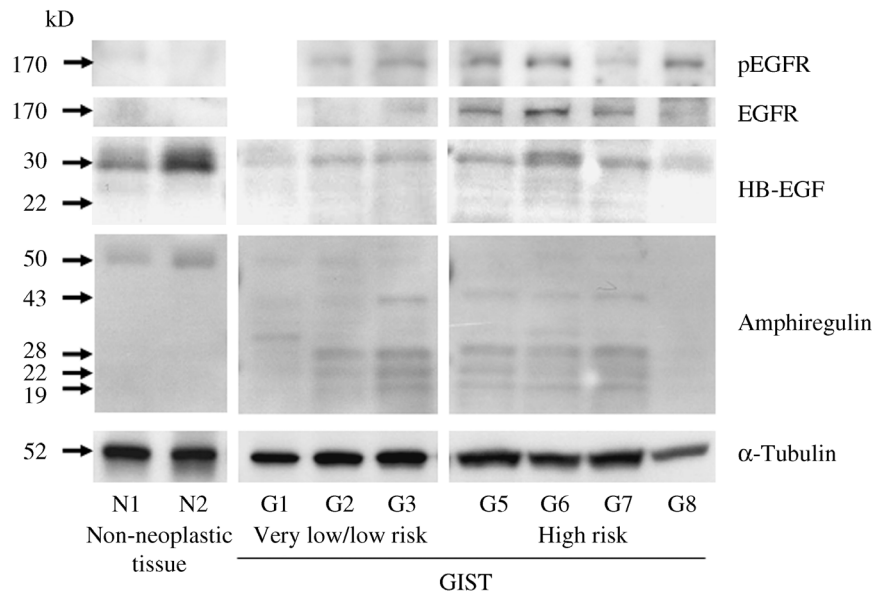


Fig. 6. Immunoblot analysis of phosphorylated epidermal growth factor receptor (pEGFR), heparin binding epidermal growth factor-like growth factor (HB-EGF), and amphiregulin. Tissue extracts were subjected to immunoblot analysis with antibodies to EGFR, pEGFR, HB-EGF, amphiregulin, and α -tubulin, as described in the Materials and Methods section. Bands at 170 kDa were detected for pEGFR. Clear bands at 30 kDa and faint bands at 22 kDa were demonstrated for HB-EGF. Multiple bands at 50, 43, 28, 22, and 19 kDa were obtained for amphiregulin.

tissues did not coexpress ADAM17, whereas GIST cells expressed both KIT and ADAM17. These findings support the idea that ADAM17 is up-regulated during GIST tumorigenesis.

The EGFR family consists of four closely related receptors, namely the EGFR (ErbB1/HER1), ErbB2 (HER2/neu), ErbB3 (HER3), and ErbB4 (HER4).⁽²⁵⁾ Among the EGFR species, EGFR was the most frequently expressed in the present study (73% by RT-PCR). Moreover, phosphorylated/activated forms of EGFR were detected in all the tumors examined (Fig. 6). Recently, Cai *et al.* and Lopes and Bacchi also reported immunohistochemical expression of EGFR in 33% and 96% of GIST, respectively.^(26,27) The activation of EGFR is essential for carcinogenesis and metastasis in many cancers, and EGFR is amplified and/or over-expressed in human glioblastomas, malignant melanomas, epidermoid carcinomas, and gastrointestinal, urinary, and reproductive tract malignancies.^(25,28) Moreover, it was shown that EGFR signal transactivation occurs via metalloproteinase-mediated processing of EGFR ligand precursors.⁽²⁹⁾ Recently, members of the ADAM family of metalloproteinases, such as ADAM10, 12, and 17, were identified as the sheddases required for this processing.⁽²⁰⁾

As for EGFR ligands, expressions of amphiregulin, HB-EGF, betacellulin, and epiregulin were detected in GISTs in the present study. TGF- α expression was not detected, although immunohistochemical expression of TGF- α in GISTs was reported previously.⁽²⁶⁾ The reason for this difference is currently unknown. Amphiregulin and HB-EGF have been implicated in human tumorigenesis. Amphiregulin is involved in an autocrine loop in several types of cancers, such as colon, breast, pancreas,

and hepatocellular carcinomas.^(30–32) HB-EGF is over-expressed in pancreatic, gastric, colonic, and hepatocellular carcinomas.^(33–35) Another important finding in the present study is that shed soluble forms of amphiregulin were identified in tumor extracts, indicating the presence of proteolytic processing of EGFR ligands within gastric GIST. Amphiregulin is synthesized as a 252-amino acid heparin-binding glycoprotein with an EGF-like domain.⁽³⁶⁾ Recent studies indicate that soluble (active) amphiregulin may be involved in up-regulation of MMPs and invasion by tumor cells.^(17,37) Moreover, there is considerable evidence to suggest that ADAM17 is involved specifically in amphiregulin, HB-EGF, and TGF- α cleavage.^(13,14) ADAM17-mediated shedding of these EGFR ligands is a key mechanism of sending signals to activate EGFR, leading to phosphorylation of EGFR.^(22,38) In the present study, expression of amphiregulin and HB-EGF was associated with expression of ADAM17 and pEGFR in GISTs, accompanied by detection of proteolytically cleaved soluble forms of amphiregulin. An EGFR ligand/EGFR autocrine or paracrine loop via ADAM17 may play a crucial role in the aggressive behavior of GISTs, although further investigation is needed. Targeting cleavage of amphiregulin or other EGFR ligands by ADAM17 may be effective in overcoming imatinib resistance of certain types of gastric GIST.

Acknowledgments

This work was supported in part by a Grant-in-Aid for Scientific Research (15390119) from the Ministry of Education, Culture, Sports, Science and Technology of Japan.

References

- Miettinen M, Lasota J. Gastrointestinal stromal tumors – definition, clinical, histological, immunohistochemical, and molecular genetic features and differential diagnosis. *Virchows Arch* 2001; **438**: 1–12.
- Fletcher CD, Berman JJ, Corless C *et al.* Diagnosis of gastrointestinal stromal tumors: a consensus approach. *Hum Pathol* 2002; **33**: 459–65.
- Hirota S, Isozaki K, Moriyama Y *et al.* Gain-of-function mutations of c-kit in human gastrointestinal stromal tumors. *Science* 1998; **279**: 577–80.
- Miettinen M, Lasota J. Gastrointestinal stromal tumors: review on morphology, molecular pathology, prognosis, and differential diagnosis. *Arch Pathol Laboratory Med* 2006; **130**: 1466–78.
- Heinrich MC, Corless CL, Duensing A *et al.* PDGFRA activating mutations in gastrointestinal stromal tumors. *Science* 2003; **299**: 708–10.
- Hirota S, Ohashi A, Nishida T *et al.* Gain-of-function mutations of platelet-derived growth factor receptor alpha gene in gastrointestinal stromal tumors. *Gastroenterology* 2003; **125**: 660–7.
- van Oosterom AT, Judson IR, Verweij J *et al.* Update of phase I study of imatinib (STI571) in advanced soft tissue sarcomas and gastrointestinal stromal tumors: a report of the EORTC Soft Tissue and Bone Sarcoma Group. *Eur J Cancer* 2002; **38** (Suppl 5): S83–7.
- Joensuu H, Fletcher C, Dimitrijevic S, Silberman S, Roberts P, Demetri G. Management of malignant gastrointestinal stromal tumours. *Lancet Oncol* 2002; **3**: 655–64.
- Antonescu CR, Besmer P, Guo T *et al.* Acquired resistance to imatinib in gastrointestinal stromal tumor occurs through secondary gene mutation. *Clin Cancer Res* 2005; **11**: 4182–90.
- Heinrich MC, Corless CL, Blanke CD *et al.* Molecular correlates of imatinib resistance in gastrointestinal stromal tumors. *J Clin Oncol* 2006; **24**: 4764–74.

- 11 Mochizuki S, Okada Y. ADAMs in cancer cell proliferation and progression. *Cancer Sci* 2007; **98**: 621–8.
- 12 Moss ML, Jin SL, Milla ME *et al*. Cloning of a disintegrin metalloproteinase that processes precursor tumour-necrosis factor- α . *Nature* 1997; **385**: 733–6.
- 13 Sunnarborg SW, Hinkle CL, Stevenson M *et al*. Tumor necrosis factor- α converting enzyme (TACE) regulates epidermal growth factor receptor ligand availability. *J Biol Chem* 2002; **277**: 12838–45.
- 14 Hinkle CL, Sunnarborg SW, Loiselle D *et al*. Selective roles for tumor necrosis factor α -converting enzyme/ADAM17 in the shedding of the epidermal growth factor receptor ligand family: the juxtamembrane stalk determines cleavage efficiency. *J Biol Chem* 2004; **279**: 24179–88.
- 15 Wikstrand CJ, Hale LP, Batra SK *et al*. Monoclonal antibodies against EGFRvIII are tumor specific and react with breast and lung carcinomas and malignant gliomas. *Cancer Res* 1995; **55**: 3140–8.
- 16 Umata T, Hirata M, Takahashi T *et al*. A dual signaling cascade that regulates the ectodomain shedding of heparin-binding epidermal growth factor-like growth factor. *J Biol Chem* 2001; **276**: 30475–82.
- 17 Brown CL, Meise KS, Plowman GD, Coffey RJ, Dempsey PJ. Cell surface ectodomain cleavage of human amphiregulin precursor is sensitive to a metalloprotease inhibitor. Release of a predominant N-glycosylated 43-kDa soluble form. *J Biol Chem* 1998; **273**: 17258–68.
- 18 McCulloch DR, Harvey M, Herington AC. The expression of the ADAMs proteases in prostate cancer cell lines and their regulation by dihydrotestosterone. *Mol Cell Endocrinol* 2000; **167**: 11–21.
- 19 Yoshimura T, Tomita T, Dixon MF, Axon AT, Robinson PA, Crabtree JE. ADAMs (a disintegrin and metalloproteinase) messenger RNA expression in *Helicobacter pylori*-infected, normal, and neoplastic gastric mucosa. *J Infect Dis* 2002; **185**: 332–40.
- 20 Gschwind A, Hart S, Fischer OM, Ullrich A. TACE cleavage of proamphiregulin regulates GPCR-induced proliferation and motility of cancer cells. *Embo J* 2003; **22**: 2411–21.
- 21 Tanaka Y, Miyamoto S, Suzuki SO *et al*. Clinical significance of heparin-binding epidermal growth factor-like growth factor and a disintegrin and metalloprotease 17 expression in human ovarian cancer. *Clin Cancer Res* 2005; **11**: 4783–92.
- 22 Peschon JJ, Slack JL, Reddy P *et al*. An essential role for ectodomain shedding in mammalian development. *Science* 1998; **282**: 1281–4.
- 23 Mann GB, Fowler KJ, Gabriel A, Nice EC, Williams RL, Dunn AR. Mice with a null mutation of the TGF α gene have abnormal skin architecture, wavy hair, and curly whiskers and often develop corneal inflammation. *Cell* 1993; **73**: 249–61.
- 24 Threadgill DW, Dlugosz AA, Hansen LA *et al*. Targeted disruption of mouse EGF receptor: effect of genetic background on mutant phenotype. *Science* 1995; **269**: 230–4.
- 25 Normanno N, De Luca A, Bianco C *et al*. Epidermal growth factor receptor (EGFR) signaling in cancer. *Gene* 2006; **366**: 2–16.
- 26 Cai YC, Jiang Z, Vittimberga F *et al*. Expression of transforming growth factor- α and epidermal growth factor receptor in gastrointestinal stromal tumours. *Virchows Arch* 1999; **435**: 112–15.
- 27 Lopes LF, Bacchi CE. EGFR and gastrointestinal stromal tumor: an immunohistochemical and FISH study of 82 cases. *Mod Pathol* 2007; **20**: 990–4.
- 28 Salomon DS, Brandt R, Ciardiello F, Normanno N. Epidermal growth factor-related peptides and their receptors in human malignancies. *Crit Rev Oncol Hematol* 1995; **19**: 183–232.
- 29 Prenzel N, Zwick E, Daub H *et al*. EGF receptor transactivation by G-protein-coupled receptors requires metalloproteinase cleavage of proHB-EGF. *Nature* 1999; **402**: 884–8.
- 30 Johnson GR, Saeki T, Gordon AW, Shoyab M, Salomon DS, Stromberg K. Autocrine action of amphiregulin in a colon carcinoma cell line and immunocytochemical localization of amphiregulin in human colon. *J Cell Biol* 1992; **118**: 741–51.
- 31 Funatomi H, Itakura J, Ishiwata T *et al*. Amphiregulin antisense oligonucleotide inhibits the growth of T3M4 human pancreatic cancer cells and sensitizes the cells to EGF receptor-targeted therapy. *Int J Cancer* 1997; **72**: 512–17.
- 32 Castillo J, Erroba E, Perugorria MJ *et al*. Amphiregulin contributes to the transformed phenotype of human hepatocellular carcinoma cells. *Cancer Res* 2006; **66**: 6129–38.
- 33 Inui Y, Higashiyama S, Kawata S *et al*. Expression of heparin-binding epidermal growth factor in human hepatocellular carcinoma. *Gastroenterology* 1994; **107**: 1799–804.
- 34 Kobrin MS, Funatomi H, Friess H, Buchler MW, Stathis P, Korc M. Induction and expression of heparin-binding EGF-like growth factor in human pancreatic cancer. *Biochem Biophys Res Commun* 1994; **202**: 1705–9.
- 35 Ito Y, Higashiyama S, Takeda T, Okada M, Matsuura N. Bimodal expression of heparin-binding EGF-like growth factor in colonic neoplasms. *Anticancer Res* 2001; **21**: 1391–4.
- 36 Plowman GD, Green JM, McDonald VL *et al*. The amphiregulin gene encodes a novel epidermal growth factor-related protein with tumor-inhibitory activity. *Mol Cell Biol* 1990; **10**: 1969–81.
- 37 Kondapaka SB, Fridman R, Reddy KB. Epidermal growth factor and amphiregulin up-regulate matrix metalloproteinase-9 (MMP-9) in human breast cancer cells. *Int J Cancer* 1997; **70**: 722–6.
- 38 Borrell-Pages M, Rojo F, Albanell J, Baselga J, Arribas J. TACE is required for the activation of the EGFR by TGF- α in tumors. *Embo J* 2003; **22**: 1114–24.
- 39 Kodama T, Ikeda E, Okada A *et al*. ADAM12 is selectively overexpressed in human glioblastomas and is associated with glioblastoma cell proliferation and shedding of heparin-binding epidermal growth factor. *Am J Pathol* 2004; **165**: 1743–53.
- 40 Grant GM, Cobb JK, Castillo B, Klebe RJ. Regulation of matrix metalloproteinases following cellular transformation. *J Cell Physiol* 1996; **167**: 177–83.
- 41 Honda M, Mori M, Ueo H, Sugimachi K, Akiyoshi T. Matrix metalloproteinase-7 expression in gastric carcinoma. *Gut* 1996; **39**: 444–8.
- 42 Lampert K, Machein U, Machein MR, Conca W, Peter HH, Volk B. Expression of matrix metalloproteinases and their tissue inhibitors in human brain tumors. *Am J Pathol* 1998; **153**: 429–37.
- 43 Nakada M, Nakamura H, Ikeda E *et al*. Expression and tissue localization of membrane-type 1, 2, and 3 matrix metalloproteinases in human astrocytic tumors. *Am J Pathol* 1999; **154**: 417–28.
- 44 Adam RM, Borer JG, Williams J, Eastham JA, Loughlin KR, Freeman MR. Amphiregulin is coordinately expressed with heparin-binding epidermal growth factor-like growth factor in the interstitial smooth muscle of the human prostate. *Endocrinology* 1999; **140**: 5866–75.
- 45 Aoki M, Nabeshima K, Koga K *et al*. Imatinib mesylate inhibits cell invasion of malignant peripheral nerve sheath tumor induced by platelet-derived growth factor-BB. *Laboratory Invest* 2007; **87**: 767–79.
- 46 Patel NV, Acarregui MJ, Snyder JM, Klein JM, Sliwkowski MX, Kern JA. Neuregulin-1 and human epidermal growth factor receptors 2 and 3 play a role in human lung development *in vitro*. *Am J Respir Cell Mol Biol* 2000; **22**: 432–40.